Measurement of relative levels of radioactivity in labelled tissue sections using image analysis

R. ORD, A. HODGES, A. NIXON, A. MOLENAAR, P. DOBBIE AND S. KIRK

AgResearch, Ruakura Agricultural Centre, Private Bag, Hamilton New Zealand.

ABSTRACT

The detection of small amounts of biologically active material in animals may require quantification of radioactive label. Here we compare several image analysis methods for quantifying relative levels of radioactive probe detected by x-ray film or photographic emulsion. Total RNA "dot blots" and ovine muscle sections were probed for the presence of muscle actin mRNA using ^{35}S-labelled riboprobes. Bound probe was detected by x-ray film in both cases. The probed sections were further exposed to photographic emulsion, while the dot blots were individually quantified by scintillation counting. Bound probe was quantified macroscopically by digitisation of optical density (OD) and thresholding of the x-ray film image. Dot blot image ODs were correlated with scintillation counts ($r > 0.96$), demonstrating that the levels of mRNA detected in tissues by autoradiography are proportional to cellular mRNA concentration. Densitometry of section macroautoradiographic images can therefore be useful in determining relative probe signal at the tissue level. When probe was quantified microscopically by counting silver grains in emulsion autoradiographs, simple thresholding correlated with manual counts ($r = 0.88$) but was unreliable at higher grain densities. Processing of the gray image gave a more direct estimate of silver grain density ($r = 0.98$).

Keywords: autoradiography, image, probe, quantitation.

INTRODUCTION

The visualisation of small amounts of biologically active material in animal tissues using radioactive probes and autoradiography has been largely qualitative, with a subjective assessment of the amount of signal. However, computer assisted image analysis, a powerful tool for examining video, photographic or autoradiographic images (Ramm, 1990; Huijsmans *et al*, 1986; Russ, 1990), now makes quantitative autoradiography possible.

Where the probed material is effectively two-dimensional (bound to filters or in tissue sections), bound probe can be visualised with x-ray film or autoradiographic emulsion placed in close contact with the material. This produces images of localized probe at the macroscopic level, or silver grains at the microscopic level (Stein and Yanishevsky, 1979). The transmission of light through such images allows their "capture" by the digitization of signals from light detectors such as video cameras or densitometers, for computer assisted quantitation. For x-ray film images the inverse of the transmission, optical density (OD) of the captured image is usually measured. Whereas the OD of macroscopic x-ray film images estimates levels of bound probe attributable to silver grains over a large area of section (see "Autoradiographic Detection Principles", Eastman Kodak Co.), the estimation of local levels of probe bound in a tissue can often only be accomplished by counting grains. In this case, image analysis can also be used to detect silver grains at the microscopic level. If all grains in the 3-dimensional emulsion layer can be resolved at a particular magnification, then their number can be estimated.

Here, we first sought to correlate sulfur-35 (^{35}S) labelled actin mRNA probe bound to dot blots of muscle (total) RNA, as detected by scintillation counts, with the mean OD of x-ray film images from the same blots. Next we wanted to compare these dot blot x-ray film image ODs with x-ray film image ODs of muscle sections from the same animals, probed *in situ* with the same actin RNA probe. Finally, we wanted to compare different computer-assisted methods, for OD estimates at the macroscopic level, or for estimating silver grain density at the microscopic level in photographic emulsion applied to the sections.

MATERIALS AND METHODS

Actin mRNA was detected via dot blot and *in situ* hybridisation (ISH) using a human ^{35}S-labelled ß-actin antisense riboprobe (Wilkins *et al*, 1989). ^{35}S-UTP was incorporated into both sense and antisense actin riboprobes (see Ord and Callaghan, this issue) and the sense probe was used as a control for non-specific probe binding.

Ovine muscle (*M.biceps femoris*) was isolated from several animals (Hua *et al*, 1993) and either frozen in liquid nitrogen and stored at -60°C for RNA extraction, or fixed in 10% formalin/phosphate buffered saline, paraffin-embedded and sectioned.

ISH of probe to tissue sections was essentially as described by Molenaar *et al*, (1992) and Hodges (1992), except that hybridisations were performed at 45°C. Macroautoradiographs were obtained by apposing X-ray film (Kodak X-Omat AR5; without preflashing) to the sections for several days. Slides were then coated with emulsion (Ilford K5, diluted 1:1 with water) and developed after appropriate times as estimated from the macroautoradiographs, usually several weeks, then counterstained with haematoxylin and eosin.

Total RNA was used for dot blot analysis so that the same population of RNAs was probed as with ISH. RNA was isolated from frozen muscle tissue using a procedure similar to that of Chomczynski and Sacchi (1987). RNA was applied to a charged nylon membrane ('dot blot'; described in the legend to Figure 1). Prehybridisation and hybridisation were at 67°C and followed a modification of the procedure of Church and Gilbert (1984). The probed blots were exposed to x-ray film, stained with Methylene Blue to detect RNA, cut into sections and the counts per minute (CPMs) for individual dots were determined in a Beckman scintillation counter.

For capturing macroautoradiographic (x-ray film) images, part or all of a 20 X 25 cm X-ray film was scanned with a Molecular Dynamics Personal laser (transmission) densitometer. Images were either quantitated directly in the densitometer's computer using the application IMAGEQUANT, or TIFF files of the images were transferred to an Apple Macintosh MacII computer and quantitated with the freeware NIH application IMAGE (versions 1.37-1.43). Mean image ODs (0-4) were expressed as 12 bit pixel densities (0-4096) in IMAGEQUANT, and as 8-bit gray levels of 1-255 in IMAGE. Specific binding of probe was determined by subtracting the mean pixel density of the control probe from that of the actin mRNA probe. The integrated density (ID or 'volume') of dot blot images was obtained by multiplying the area of the image in pixels by its mean pixel density after correction for background (see text). Care was taken to exclude tissue folds and other artifacts when quantitating the scanned ISH sections.

The ODs of XAR film were ≈ 0.05 if exposed to daylight with both side's emulsion layers stripped off, ≈ 1.33 with one side's emulsion stripped off, and ≈ 2.72 with both side's emulsion layers intact (the normal situation). Since the images generated with the low energy ^{35}S electron would be largely confined to one side of the double-sided XAR film, the second value OD ≈ 1.33) therefore represents the maximum ^{35}S OD measurable.

The mean section image OD (gray level) was determined by "thresholding" (selecting the range of pixel densities to be measured; McKanna and Casagrande, 1985) the entire image of an individual section or dot, in the IMAGE application. Alternatively, five random sites on a tissue section image (7 X 7) pixel squares were measured and averaged (Figure 7; Hodges, 1992). In the latter experiments ovine muscle sections were probed with a human IGF-I ^{35}S riboprobe rather than actin (the principal, method and nuclide used were identical). The criteria for accepting the randomly selected area was that it was completely positioned on the section image and that the standard deviation of the mean density was less than 5.0. A standard deviation of greater than 5.0 was taken to indicate that the selected area was not of homogeneous density due to an artifact.

Microautoradiographs were viewed at 400x magnification and video images were captured and analysed using either "VISILOG" (Noesis) software on an IBM compatible 386 computer, or IMAGE (NIH) on an Apple Macintosh IIfx. In muscle sections from four animals, the density of silver grains was measured microscopically at ten randomly chosen sites in the sections probed for actin mRNA and ten corresponding sites in the control sections. The area of each site was determined and silver grains counted by: (i) manual counts of grains on the video screen, (ii) thresholding and counting discrete objects in the binary image; and (iii) gray image processing to find local intensity maxima, using the "regional extrema" command available in "VISILOG".

Regression statistics including "r", "RSD" (residual standard deviation) and "p" (F-test probability) were calculated using the application "STATVIEW II".

RESULTS

Correlation of ^{35}S radioactivity with x-ray film image OD for probe quantitation in tissue sections

The mean optical densities of dot blot images for ^{35}S UTP labelled probe bound to 1, 3.3 and 10 µg dots of total muscle RNA (Figure 1, top) and captured by a transmission (laser) densitometer with IMAGEQUANT were plotted against CPM. As expected, CPM but not OD increased linearly with ug of RNA loaded (data not shown), and OD varied non-linearly with CPM (Figure 2A). However, the 10 µg dot values approximated a linear distribution over the small OD range (Figure 2B).

FIGURE 1: **TOP:** Dot blot hybridizations of a ^{35}S-labelled actin riboprobe with total ovine muscle RNA isolated from twenty sheep loaded in 10, 3.3 and 1 µg quantities. The dots in the seventh column are from control hybridizations with actin cDNA. Except for Figure 2A, only the 10 µg dot values (columns 1 and 4) were used. **BOTTOM:** *In situ* hybridizations of the riboprobe with actin RNA in ovine muscle sections from the same animals. The picture is overexposed to demonstrate the non-specific probe binding to control sections seen faintly above each experimental section. The gray level of each control section was subtracted from its corresponding experimental section, then these values from the two duplicate samples were averaged to obtain the mean gray level value.

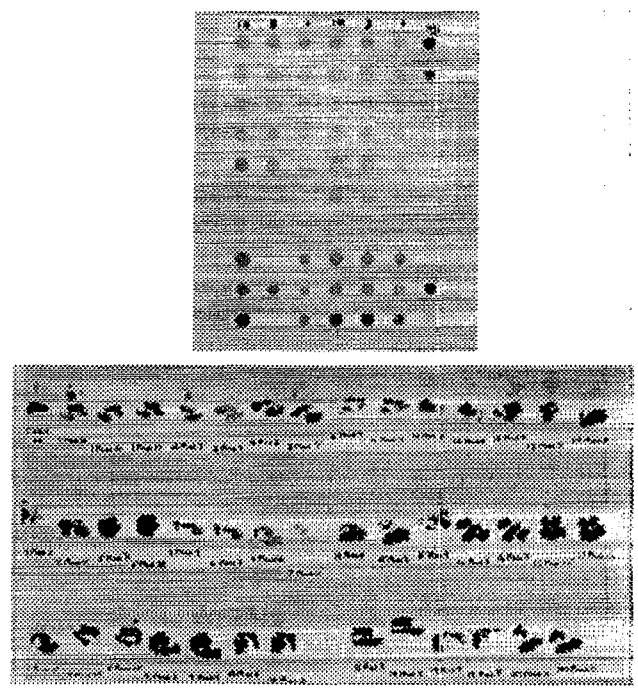

To make a meaningful comparison with scintillation counts, it was necessary to subtract the high background OD.

After subtraction of a measured background (≈0.12), we then compared the directly measured OD shown in Figure 2B with the same image converted from 12 to 8 bits/pixel and measured as gray levels using IMAGE (Figure 2C). The OD values (Fig. 2B, r = 0.936) were very similar to the graylevels (Fig. 2C, r = O.917). The relationship of OD or gray level with CPM was effectively linear over the range examined, but wasn't 1:1 in either case.

Integrated densities ('volumes') should be more directly proportional to CPM, since the values obtained correct for the differences in radioactive "dot" area. In this case the volume measurements for the laser images were approximately 1:1 relative to CPM (Figure 2D, measured by thresholding in IMAGE).

Finally, the dot blot image (Figure 1, top) gray levels were correlated with image gray levels from serial sections (Figure 1, bottom) also probed with ^{35}S-labelled actin RNA (measured using IMAGE). Integrated densities weren't compared because the serial sections were of different sizes. As shown in Figure 2E, muscle actin mRNA levels determined using ISH were proportionately similar to actin mRNA levels in total muscle RNA (r = 0.866, p = 0.0025; Note that 10/19 images in this experiment from a separate group treated with growth hormone (Hua *et al*, 1993) were not similarly correlated, and were excluded).

Comparison between x-ray film images using two "capture and analysis" methods

The thresholding method (demonstrated in Figures 2C, D and E) to calculate the mean pixel density of an entire section from x-ray film yielded results similar to a method which measured small, randomly generated areas within the section image (Figure 3; r = 0.904; the second method used a flatbed scanner for the generation of the image).

Comparison of grain counting methods in micro-autoradiographs

Silver grain densities representing actin mRNA in muscle were determined microscopically from the difference between total (antisense) and non-specific (sense) probed sections, for several of the sections shown in Figure 1 (bottom). Grain densities calculated from counts made using

FIGURE 2: Correlations of dot blot x-ray film images.

A. Non linear relationship of probe detected in dot blots of 10, 3.3 and 1 µg aliquots of total ovine muscle RNA, detected by scintillation counts (CPM) vs. x-ray film OD determined by laser densitometry using the application IMAGEQUANT.

y = 6.08E4 - 9.16E5x + 3.49E6x2 r = 0.904
p = 0.0001 RSD = 620

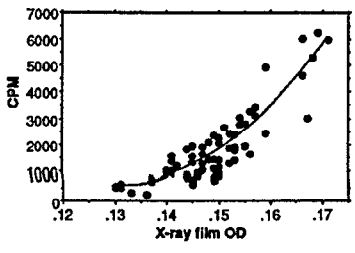

B. Linear regression of dot blot CPMs with OD for 10ug dots from Fig. 4A (varying from OD 0.14 to 0.17). Note the OD 'window' containing useful information. The sample showing the weakest signal was found to have degraded RNA, and was excluded in the figures below.

y = 1.65E5x - 2.23E4 r = 0.936
p = 0.0001 RSD = 672

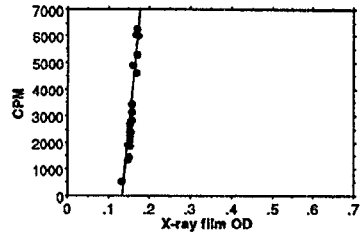

C. Dot blot CPMs from Fig. 4B compared with dot blot gray levels determined using IMAGE, by 'thresholding' 8 bit images after converting ODs 0.12-2.5 to 256 grays with the equation:

$$\text{8 bit value} = \frac{\text{Scanned 12-bit value} \times 256}{\text{Max 12-bit value - min 12-bit value}}$$

where 'max' and 'min' are the highest and lowest pixel densities chosen to convert from 12 bit to 8 bit (12-bit value ≈ actual OD X 1000; CONVERT application, Molecular Dynamics Ltd).

y = 200x - 3878 r = 0.917
p = 0.0001 RSD = 491

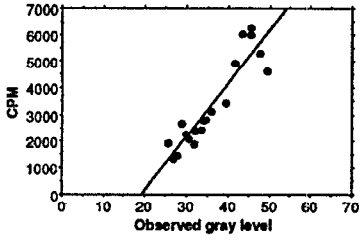

D. Correlation of actin mRNA levels per 10ug of total RNA detected as CPM (corrected for background counts), with 8-bit integrated densities ('volume' = gray level x area) of the dot blot image ODs given in Fig. 4C, made using IMAGE.

y = 0.11x - 329 r = 0.957
p = 0.0001 RSD = 491

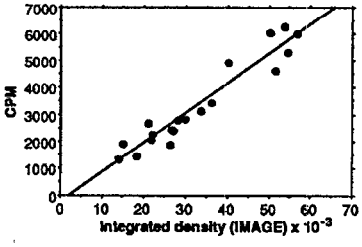

E. Correlation of actin mRNA levels per 10µg of total RNA detected via dot blotting, with actin mRNA levels in muscle sections detected via in situ hybridization.

y = 0.27x - 26.33 r = 0.866
p = 0.0025 RSD = 3.49

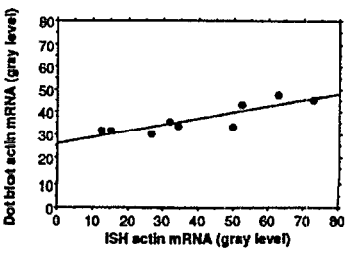

FIGURE 3: Comparison of two computer assisted methods used to estimate mean pixel density of bound probe on muscle sections. Analysis 'A' estimated mean pixel density of a section from five separate determinations (see text). Analysis 'B' estimated mean pixel density of the entire image by thresholding. This graph represents ontogeny of IGF-I mRNA in sheep skeletal muscle. The image analysis data (B) is expressed as a percentage of the maximum value.

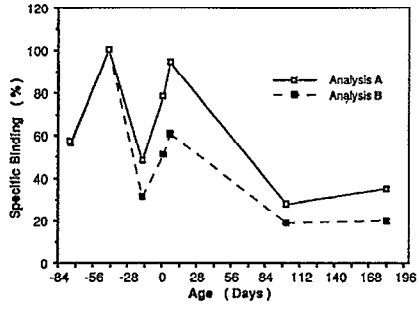

FIGURE 4: Correlation of silver grain densities in micro-autoradiographs determined by manual counting, with computer assisted methods. A. simple thresholding; B. thresholding and finding local minima by gray image dilation.

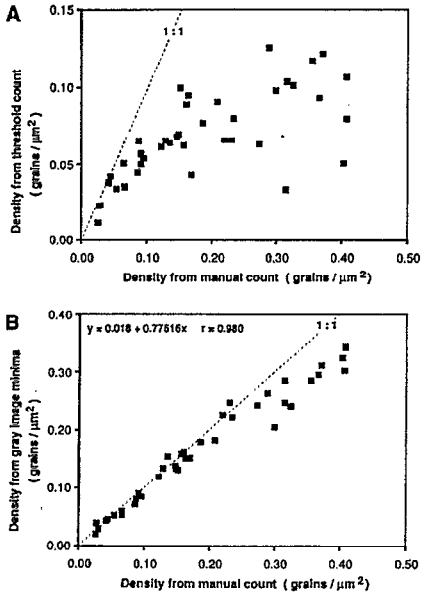

operator adjusted thresholding correlated significantly with density from manual counts (Figure 4A; r=0.88). However, the relationship was non-linear, and uncorrelated above 0.1 grains/µm². By setting a threshold to include all silver grains and finding regional minima within this mask by a series of gray image erosions, a more direct estimate of the apparent silver grain density (Figure 4B; r=0.99; RSD = 0.0189) was obtained.

DISCUSSION

The levels of ^{35}S-labelled actin mRNA detected in muscle sections by autoradiography were highly correlated with the concentration of actin mRNA in total muscle RNA detected by scintillation counting. Densitometry of macroautoradiographs can therefore be useful in determining relative probe signal at the tissue level.

X-ray film which has not been pre-flashed has a restricted OD range which is linear with CPM (Eastman Kodak Co.; 1989). However, this difficulty can be circumvented by selecting a small change in x-ray film OD to calibrate against CPM. In this study, experiments were performed by taking such a window of ODs which just covered the experimental range (usually from the background x-ray film density (OD 0.05-0.2) to OD 0.3-1.5). In this case the change in signal was effectively linear but less than a 1:1 ratio with changes in CPM. Hence a calibration should be performed to avoid underestimation of real differences.

Where radioactivity is relatively homogeneous in a tissue section the quantitation of a mean image OD or gray level using the thresholding method is faster than a "random coordinates" method although the latter is valuable where numerous areas must be excluded. Images of tissues such as mammary gland having regions of variable signal will likely need further processing.

For the quantitation of silver grains at the microscopic level, it is clear from Figure 4 that simply thresholding and counting detected objects (eg. McKanna and Casagrande,1985) is unreliable at higher grain densities due to merging of detected objects. However, by finding local minima by gray image dilation (McMillan *et al*, 1987), most of the silver grains were detected and separated over a wide density range, as indicated by the near-linear relationship with manual counts. Note that choice of method for image analysis of micro-autoradiographs also depends on various factors not seen at the "macro" level, including evenness of image background, absolute grain density, cell type heterogeneity, between-sample variation, and convenience of use.

REFERENCES

Chomczynski, P. and Sacchi, N. (1987). Single-step method of RNA isolation by acid guanidinium thiocyanate-phenol-chloroform extraction. *Anal. Biochem.* **162:** 156-159.

Church, G.M. and Gilbert, W. (1984). Genomic Sequencing. *Proc. Natl. Acad. Sci.* **81:** 1991-1995.

Eastman Kodak Co. (1989) Autoradiographic Detection Principles (handbook available from Kodak).

Hodges, A.K. (1992) Developmental change and histological localization of insulin-like growth factor I and insulin-like growth factor II mRNA in muscle and liver tissue of sheep. M.Sc. Thesis. Waikato University Dept.of Biology.

Hua, K.M.; Ord, R.; Kirk, S.; Hodgkinson, S.C.; Spencer, G.S.G.; Molan, P.C.; and Bass, J.J. (1993). Regulation of plasma and tissue insulin-like growth factor-I levels by nutrition and growth hormone in sheep. *J. Endocrinology.* **136:** 217-224.

Huijsmans, D.P.; Lamers, W.H.; Los, J.A. and Strackee, J. (1986). Toward computerized morphometric facilities: a review of 58 software packages for computer-aided three-dimensional reconstruction, quantification, and picture generation from parallel serial sections. *Anatomical record.* **216:** 449-470.

McKanna, J.A. and Casagrande, V.A. (1985). Computerized radiographic grain counting. *In:*The microcomputer in cell and neurobiology research. R. Ranney Mise (ed.) Elsevier, N.Y.

McMillan, P.J.; Yakash, A.; Frykman, G.; Nam, P.B. and Ras, V.R. (1987). Minimum equalization: a strategy in automatic processing of microscopic images. *J. Microscopy.* **148:** 253-262.

Molenaar, A.J.; Davis, S.R. and Wilkins, R.J. (1992). Expression of alpha-lactalbumin, alpha-S1-casein, and lactoferrin genes is heterogeneous in sheep and cattle mammary tissue. *J. Histochem. Cytochem.* **40:** 611-618.

Ramm, P. (1990). Image analysis for bioscience. *Computerised Medical Imaging and Graphics.* **14:** 287-306.

Russ, J.C. (1990). Computer-assisted microscopy: the measurement and analysis of images. Plenum Press, N.Y.

Stein, G.H. and Yanishevsky, R. (1979). Autoradiography. in Methods *In* Enzymology, LVIII [22]. Academic Press.

Wilkins, R.J.; Molenaar, A.J.; Ohlsson, R.; Reeve, A.E.; Yun, K. and Becroft, D.M.O. 1989. Wilm's Tumorigenesis, insulin-like growth factor II gene expression, and blocked differentiation. *In:* Cancer Cells 7/ Molecular Diagnostics of Human Cancer. Press Cold Spring Harbor N.Y.